An Improved Microslip Model
for Variable Normal Loads

Chiara Gastaldi and Muzio M. Gola

Abstract Detuning of gas turbine blades in order to avoid high cycle fatigue failure due to large resonant stresses is often unfeasible. A possible solution is to add an external source of damping, in the form of dry friction devices such as the under-platform damper. The relative movement between the blades causes possible slip between damper and blade surfaces. Due to the nonlinear nature of dry friction, dynamic analysis of structures constrained through frictional contacts is difficult, commercial finite element codes using time step integration are not suitable given the large computation times. For this reason, ad hoc numerical codes have been developed in the frequency domain. Some authors Yang and Menq (J Eng Gas Turbine Power 120:410–417, 1998) [1], Sanliturk et al. (J Eng Gas Turbine Power 123:919–929, 2001) [2], Csaba (Proceeding of ASME Gas turbine and aeroengine congress and exhibition) [3], Panning et al. (Int J Rotating Mach 9:219–228, 2003) [4] prefer a separate routine in order to compute contact forces as a function of input displacements, others Cigeroglu et al. (J Eng Gas Turbine Power 131:022505, 2009) [5], Firrone et al. (Modelling a friction damper: analysis of the experimental data and comparison with numerical results, 2006) [6], Firrone and Zucca (Numerical analysis—theory and application, 2011) [7] include the damper in the FE model of the bladed array. The available numerical models of dampers require a description of the contact conditions, both in the normal and in the tangential directions. The approach proposed here differs from those available in the literature in that the tangential force-displacement behaviour is described by arrays of springs in parallel, but, unlike pre-existing models, it introduces a variable sharing of normal force according to the approach along the normal. It thus modulates the tangential stick-slip capabilities according to normal force and approach and is capable to reproduce the analytical contact description as originally proposed by Cattaneo (Accademia dei Lincei 6:P I; 342–348, P II; 434–436, P III; 474–478, 1938) [8] and Mindlin and Deresiewicz (J Appl Mech 20:327–344, 1953) [9].

C. Gastaldi · M.M. Gola (✉)
Politecnico di Torino, Turin, Italy
e-mail: muzio.gola@polito.it

C. Gastaldi
e-mail: chiara.gastaldi@polito.it

The paper shows how the model can be described and tuned in reference to the analytical Cattaneo and Mindlin's benchmark for a spherical contact. It is proved that parameters tuned for a certain normal load will correctly simulate the tangential behaviour at any other lower normal load and finally that the transitions between cycles at different normal loads is correctly described. The paper further shows an application to a cylindrical contact where the tangential characteristics are derived from purposely taken experimental measurements.

1 Introduction

In the frame of damper design the main object in the literature is the development of a calculation procedure that integrates blades FE model, rigid body model of the damper and contact model in order to predict the damper performance through the solution of the nonlinear dynamic response of the system. In technical literature, the problem of modeling periodical contact forces at friction contacts has been addressed by several authors, leading to different contact models.

The first macroslip model used in friction dampers was proposed by Griffin [10] in 1980. It consists of a Coulomb point contact in series with a tangential spring, and yields a simple bilinear hysteresis loop. In 1998 Yang [1] introduced normal load variation and an associated normal contact stiffness. The model was then extended to include 2D motion on the contact plane [11]. The greatest advantage of the macroslip model is the low number of parameters required for its tuning, however microslip effects have to be taken into account in case of small relative displacements or large normal loads.

An important contribution to friction interfaces modeling was given in 1938 by Cattaneo [8], who starting from Hertz [12] theory of normal contact of ellipsoids, extended it to a case of two elastic spheres in contact under the action of a constant normal force and a constant tangential force less than that of (Coulomb) limiting friction. Cattaneo showed that the effect of a tangential force smaller than the limiting friction force is to cause small relative motion, referred to as "microslip" over a part of the interface, while the rest of the contact surface deforms without relative motion, a condition referred to as "stick". This microslip contact problem was further explored by Mindlin [9], who extended it to the case of periodically applied tangential loads. Experimental studies that support the theory have been reported by Mindlin [13], Johnson [14], and Goodman and Brown [15].

Menq et al. [16] in 1986 presented a simple 1D microslip model in which an elastic bar having a uniform normal load is in contact with the rigid ground by means of a layer of springs. Sanliturk et al. [2] presented a microslip contact model constituted by an array of macroslip elements without normal contact stiffness and applied it to a wedge damper. The model is tuned against experimentally observed hysteresis loops however, given its lack of normal contact stiffness, presents no

direct connection with the damper kinematics and excludes any relation between normal force and number of macroslip elements in contact.

A different approach to model microslip requires instead the discretization of the contact area. Csaba [3], used a discretized version of the Winkler elastic foundation model, within the assumption of local friction law, to model a curved damper. The contact area is discretized and each portion is assigned a uniform normal and a tangential stiffness with equal unloaded length and different gap vectors depending on the contact area's geometry. Discretization of the contact area to model cylindrical and wedge-shaped dampers was proposed by Panning et al. [4]. In both cases the total normal and tangential stiffnesses are nonlinearly dependent on the normal relative displacements due to an increasing percentage contact area with higher normal forces. This approach has the advantage of being adaptable to any contact surface, however it introduces the simplification which sees each spring, corresponding to one point of the contact area, as decoupled from the other points. It is therefore impossible to mimic, at the same time, the same contact area and the same maximum pressure as the Hertzian solution [3].

In order to model the microslip behavior of friction contacts in FE numerical simulations of frictionally damped structures, other authors [5, 7], instead of using a separate routine to calculate the hysteresis loop, integrate the algorithm into the FE code by dividing the contact area as a grid made of several contact elements. The contact parameters (tangential and normal contact stiffness) are evaluated for the whole contact by using simplified test arrangements and their value is evenly distributed among the contact nodes. It is important to notice how this method allows for the slipping area to grow inward, even if with a different pattern from the one predicted by Cattaneo and Mindlin [7].

The model proposed in this paper is a point contact model, therefore no assumption on the contact area and subsequent discretization is performed. A parallel array of macro-slip elements with normal and tangential stiffness is used to simulate microslip. Each macroslip element is assigned its own set of contact stiffness values and normal gap vector in order to ensure a variable distribution of normal load as well as a progressive slipping. The model is at first, tuned against the analytical normal and tangential characteristic curves for a sphere pressed against a plane [8, 9] to show its robustness and internal coherence. It will be shown how the model, tuned against a hysteresis curve for a given normal load, is capable of correctly reproducing the corresponding hysteresis curves at different normal loads and the transition between them.

The model will then be tuned in the case of a cylinder pressed against a plane, this time taking as a reference experimental hysteresis curves. The cylindrical specimen has the same material and geometrical properties as the cylindrical portion of the damper tested in [17]. This will be the preferred choice whenever a reliable closed-form solution for the normal-tangential contact is not available and opens the way to the integration of the microslip model in the numerical model of the damper presented in [17].
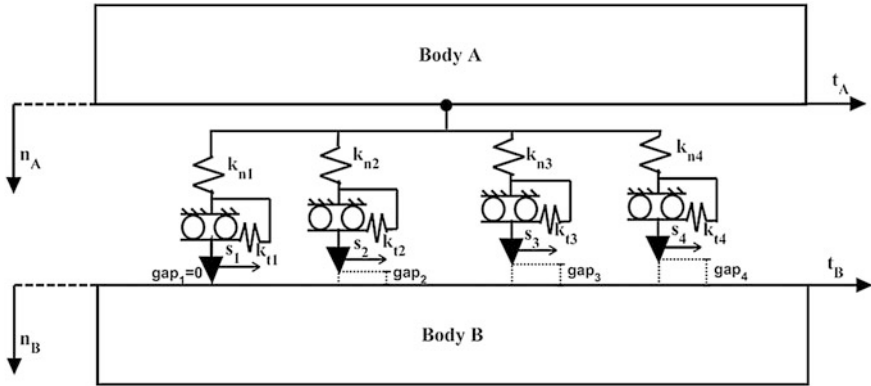
Fig. 1 Schematic view of a macroslip array of elements used to simulate microslip with variable normal load. n and t refer to the normal and tangential motion of the two bodies, while s is the motion of the slider of each macroslip element
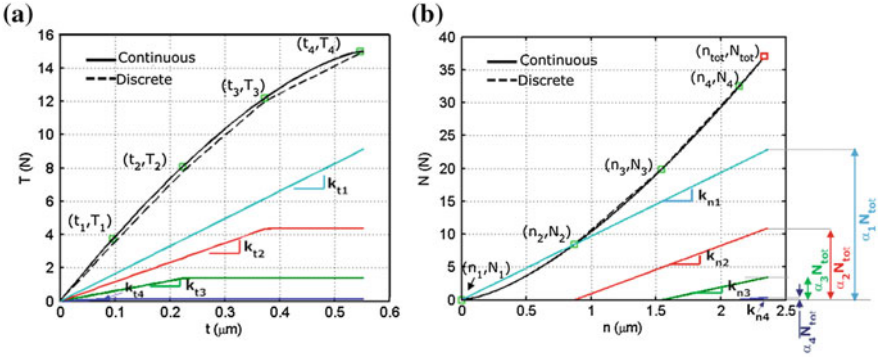
2 Benchmark: Sphere Pressed Against a Plane

The microslip model presented in this paper is based on a parallel array of macroslip contact elements shown in Fig. 1. The tuning of the value of the springs is performed against two fundamental curves, both available in a closed form for the case of a sphere pressed against a plane: (•) the tangential displacement—tangential force hysteresis curve at constant normal load; (•) the normal displacement—normal force curve.

The chosen benchmark case explores the behaviour of a sphere ($d = 10$ mm) pressed against a plane. Both are made of steel (E = 200 MPa, $v = 0.3$) and a friction coefficient $\mu = 0.4$ is assumed. In Sects. 2 and 3 the curves coming from Hertz-Cattaneo-Mindlin's theory shall be denoted as "Continuous", the simulated ones as "Discrete".

2.1 Selecting the Values of the Tangential Contact Stiffness

Using the continuous backbone ascending microslip curve, a series of J points is selected (see green markers in Fig. 2a). The same procedure could be performed on a branch of a steady hysteresis loop since Masing rules apply to the model (and this will be the case in the cylinder's characterization in Sect. 3). The tuning will ensure the resulting simulated curve to pass through the above mentioned points on the original curve. It is also essential for the last point T_4 to coincide with the value $T^* = \mu \cdot N_{tot}$, which corresponds to the value for which the model enters gross-slip. The number of points selected on the curve corresponds to the number of macroslip elements of the array: therefore it is reasonable to select an hysteresis

Fig. 2 a Ascending backbone microslip hysteresis curves for a sphere pressed against a plane with a normal force $N = 37.5$ N, b $n - N$ curves for a sphere pressed against a plane

curve taken at a relatively high level of normal load (the highest that the model will reasonably encounter, in this case referred to as N_{tot}).

Once the points on the continuous curve have been selected, it is possible to compute the values of the tangential contact stiffness that allow the discrete curve to pass through the selected points. It is assumed that the ith element enters macroslip at tangential displacement t_i. If the tangential load is $T_1 = T(t_1)$ none of the contact elements has entered macroslip, therefore it holds:

$$T_1 = \sum_{i=1}^{J} k_{ti} \cdot t_1 \tag{1}$$

While, at point i = j (with j > 1), j-1 elements are in slip, while J-j + 1 are still in stick:

$$T_j = \sum_{i=1}^{j-1} k_{tJ+1-i} \cdot t_i + \sum_{i=j}^{J} k_{tJ+1-i} \cdot t_j \tag{2}$$

In other words, referring to Fig. 2a at point (t_3, T_3), 2 springs (k_{t4} and k_{t3}) are already slipping, while k_{t2} and k_{t1} are still in stick (with k_{t2} on the point of entering gross slip). In this way it is possible to obtain a linear system of J equations with J unknowns (contact stiffness). Below an example with J = 4 is reported:

$$\begin{pmatrix} T_1 \\ T_2 \\ T_3 \\ T_4 \end{pmatrix} = \begin{bmatrix} t_1 & t_1 & t_1 & t_1 \\ t_2 & t_2 & t_2 & t_1 \\ t_3 & t_3 & t_2 & t_1 \\ t_4 & t_3 & t_2 & t_1 \end{bmatrix} \cdot \begin{pmatrix} k_{t1} \\ k_{t2} \\ k_{t3} \\ k_{t4} \end{pmatrix} \tag{3}$$

Once the tangential stiffness values have been calculated the normal load N_{tot} is distributed on the different elements so that the j-th element bears a fraction of normal load equal to

$$\alpha_j \cdot \mu \cdot N_{tot} = k_{tj} \cdot t_{J+1-j} \tag{4}$$

therefore it holds

$$\alpha_j = \frac{k_{tj} \cdot t_{J+1-j}}{\mu \cdot N_{tot}} \tag{5}$$

where α_j are the coefficients that divide the total normal load N_{tot} on the different contact elements that compose the array. They have been scaled so that the jth contact element enters macroslip at t_{J+1-j}. The sum of the coefficients $\sum_{i=1}^{J} \alpha_i = 1$, provided that $T_4 = \mu \cdot N_{tot}$, therefore the sum of the normal loads acting on the contact elements equals the total load N_{tot}.

2.2 Selecting the Values of the Normal Contact Stiffness

The calculation above only offered a repartition of load for a constant value of N_{tot}, but it does not provide a link between the approach along the normal (or normal approach) n and the normal load N_{tot}. In order to assign the normal contact stiffness the appropriate values, the normal characteristic curve $n - N$ coming from Hertz's theory is used.

Once again a number of points equal to the number of contact elements has to be selected under the assumption that at each point one of the contact elements comes into contact, therefore that its normal stiffness starts contributing to the $n - N$ curve. Two sets of quantities has to be determined:

- the values of the normal contact stiffness (k_{ni});
- the gap vector which determines for what value of normal approach each contact element comes into contact (n_i).

There are two sets of conditions that the normal contact stiffness values have to accomplish:

- ensure that, for $n = n_{tot}$ each contact element has the predefined share of normal load for the element i to slip at the right t_i. The total normal load N_{tot} can be written as (referring to Fig. 2b):

$$N_{tot} = k_{n1} \cdot (n_{tot} - n_1) + k_{n2} \cdot (n_{tot} - n_2) + k_{n3} \cdot (n_{tot} - n_3) + k_{n4} \cdot (n_{tot} - n_4) \tag{6}$$

where $n_1 = 0$. The normal load bearing on the $i - th$ element when $n = n_{tot}$ is

$$N_{tot} \cdot \alpha_i = k_{ni} \cdot (n_{tot} - n_i) \tag{7}$$

Therefore the normal contact stiffness can be written as

$$k_{ni} = \frac{\alpha_i \cdot N_{tot}}{(n_{tot} - n_i)} \tag{8}$$

- ensure the simulated $n - N$ curve to mimic the continuous curve:

$$\begin{aligned} N_2 &= k_{n1} \cdot (n_2 - n_1) \\ N_3 &= k_{n1} \cdot (n_3 - n_1) + k_{n2} \cdot (n_3 - n_2) \\ N_4 &= k_{n1} \cdot (n_4 - n_1) + k_{n2} \cdot (n_4 - n_2) + k_{n3} \cdot (n_4 - n_3) \end{aligned} \tag{9}$$

2.3 Validation

A preliminary check can be performed by observing the behaviour of the contact model when performing a complete hysteresis loop (see Fig. 3a) and when having to simulate hysteresis curves produced at normal loads different from the one the model was tuned on (see Fig. 3b). In both cases the model closely reproduces the continuous curves. The slopes are simulated with remarkable similarity, while the difference between continuous and discrete slip load is always below 8 %. This
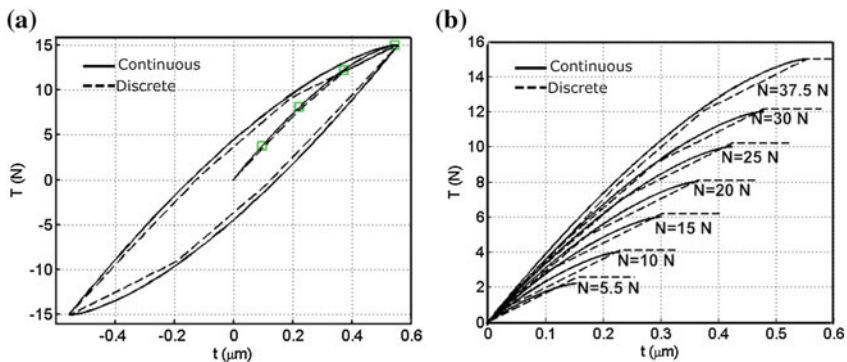
Fig. 3 **a** Continuous and discrete complete hysteresis loop at a normal load of 37.5 N and $\mu = 0.4$. The *green boxes* indicate the points used during the tuning procedure. **b** Continuous and discrete hysteresis curves at various normal loads and $\mu = 0.4$.
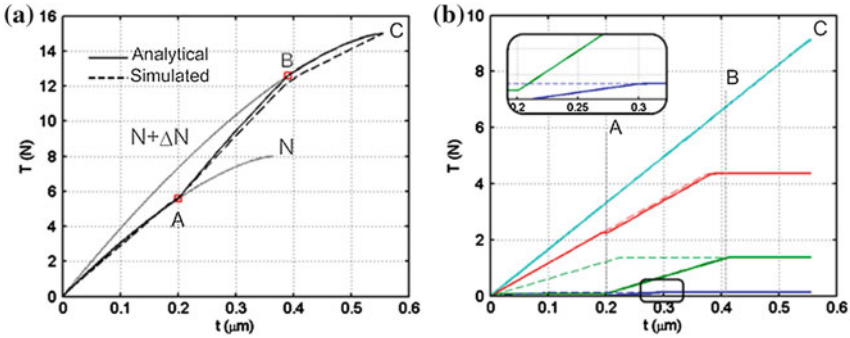
Fig. 4 a Continuous and discrete hysteresis curve for increasing N and T. **b** *Dashed lines* behaviour of each tangential spring for increasing T and a constant normal load $N + \Delta N$, corresponding to curve "O-B-C" in Fig. 4a (behaviour of all springs together). *Solid Lines* behaviour of tangential springs in case of increasing N and T, corresponding to curve "O-A-B-C" in Fig. 4a. The color code is consistent with Fig. 2a

difference is due to the discrete nature of the model and is greater for lower normal loads where, in an extreme case, only one macroslip element is used to simulate the hysteresis curve.

The model will now be tested for dynamic variations of both N and T. After an initial state has been reached (point A in Fig. 4a) by applying a normal force N and a tangential force T, N is to increase of ΔN while T keeps increasing at an arbitrary relative rate. Mindlin [9] was able to compute the displacement expression by passing through equilibrium states.

The same trend (see Fig. 4a) can be reproduced by giving to the contact model the tangential and normal displacement (t and n) thus obtained. The two levels of normal approach have been obtained by using the Hertz formula for two spheres in contact with the two values of normal load (N and $N + \Delta N$).

At point A the normal load increases by ΔN and the springs corresponding to the area which comes into contact start acting at that moment. It is worth noting that from A until element n° 4 starts slipping the overall stiffness is equal to the initial stiffness of the curve corresponding to a normal load $N + \Delta N$. Element 1 comes into contact (see zoom box in Fig. 4b) and the elements which had already begun slipping (2 and 3) are brought back to a stick condition by the increased normal load (see Fig. 4b).

Furthermore, as Mindlin pointed out, once the increment of tangential load has reached a critical value ($\Delta T = T_B - T_A = \mu \Delta N$) the curve becomes the one that would have been obtained if the normal load had been $N + \Delta N$ all along (point B in Fig. 4).

3 Experimental Characterization of a Cylinder Pressed Against a Plane

While for spherical contacts the hysteresis and normal characteristic curves are available in closed form, cylindrical contacts require experimental investigation.

The normal displacement-normal force curve has been obtained from interpolations of experimental data [18], later confirmed by Brändlein's theoretical investigations [19]. The hysteresis curve for a cylinder pressed against a plane has been measured using the already existing high-precision, high-temperature resistance flat-on-flat fretting test apparatus designed and set up by the AERMEC laboratory [20] originally dedicated to contact parameters measurement during wear process. The rig was modified to accomodate a cylindrical specimen (part C in Fig. 5c) and to avoid any relative rotation between flat and cylindrical specimens.

The cylindrical specimen (C) is connected to a fixed support (A) by means of a "seat" (B). This part has a double function, it offers a flat surface on which to point the laser measuring system and it allows to test on the same support A different cylinder geometries (different radii) by redesigning the seat. The flat specimen (D) is fixed to a mobile support, excited by a shaker.

The tangential force is measured by means of a load cell connected to support A, while the relative tangential displacement is measured by means of a laser doppler vibrometer. The tests have been operated at room temperature, at various frequencies (10–80 Hz) and increasing normal loads (16.4–36.6 N). The frequency
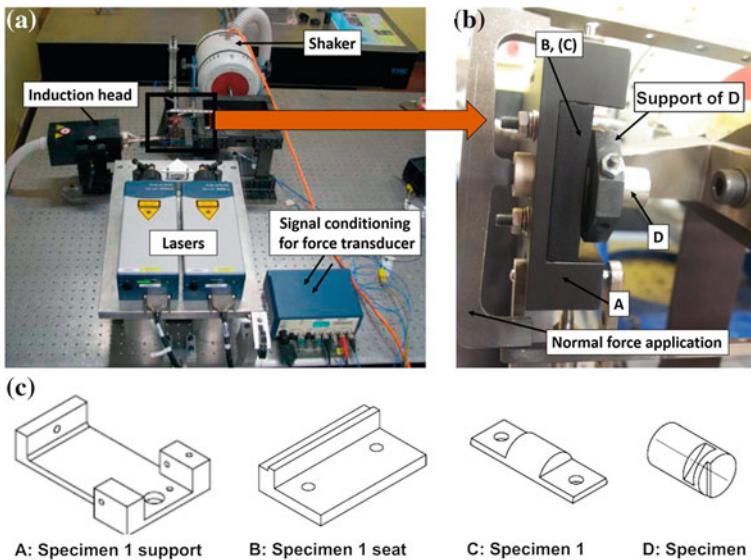
Fig. 5 Hysteresis measurement test rig: **a** general, **b** detailed view, **c** samples and samples' supports expanded view
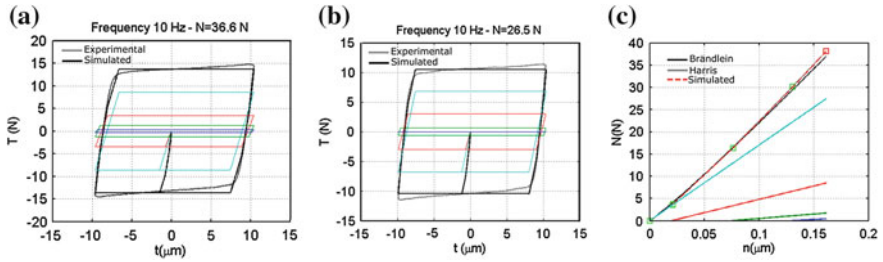
Fig. 6 **a**, **b** Hysteresis loops under different normal loads. The colored loops represent the macroslip cycles performed by each contact element, the slopes of the stick portions represent the stiffness values of each tangential spring. **c** Experimental, theoretical and simulated $n - N$ curve for a cylinder ($l = d = 10$ mm) pressed against a plane with a friction coefficient $\mu \approx 0.4$. The colored lines represent the normal springs of each contact element

had negligible effects on the hysteresis loops. The tuning of the microslip model, presented in Fig. 6a and c, has been performed, according to Sect. 2, for the highest available normal load (this time on a branch of the steady hysteresis which gives the same information as the initial loading curve since Masing's rules apply). The cylindrical specimen had the same radii of the laboratory damper investigated in [17], and was built using the same steel. It should be noted how the measured friction coefficient ($\mu \approx 0.4 - 0.45$) matches the one experimentally measured and used in the simulations in [17].

4 Conclusions

A novel microslip model capable of reproducing both the tangential microslip hysteresis loop and the normal force-normal displacement curve has been descri-bed. The presence of properly tuned normal contact stiffness and gap vectors guarantees a variable sharing of normal force according to normal approach. The practical evidence of the soundness of this model is that the model tuned for one value of normal load is capable to correctly reproduce the hysteresis loops produced at lower values of normal load. This has been proved both for a case where half space theory applies (spherical contact) and for an experimental one (cylindrical contact).

These features make this model fit to be integrated in a routine which studies the behaviour of under-platform dampers, characterized by double contact interfaces and severe normal load variations [17]. The effect of the introduction of a microslip contact model on the simulation of dynamic and kinematic behaviour of under-platform dampers is now being assessed by the authors.

References

1. Yang BD, Menq CH (1998) Characterization of contact kinematics and application to the design of wedge dampers in turbomachinery blading: part 1—Stick-slip contact kinematics. J Eng Gas Turbine Power 120:410–417
2. Sanliturk KY, Ewins DJ, Stanbridge AB (2001) Underplatform dampers for turbine blades: theoretical modelling, analysis and comparison with experimental data. J Eng Gas Turbine Power 123:919–929
3. Csaba G, Modelling of a microslip friction damper subjected to translation and rotation. In: Proceeding of ASME Gas turbine and aeroengine congress and exhibition, 99-GT-149
4. Panning L, Sextro W, Popp K (2003) Spatial dynamics of tuned and mistuned bladed disks with cylindrical and wedge-shaped friction dampers. Int J Rotating Mach 9:219–228
5. Cigeroglu E, An N, Menq CH (2009) Forced response prediction of constrained and unconstrained structures coupled through frictional contacts. J Eng Gas Turbine Power 131:022505
6. Firrone CM, Botto D, Gola MM (2006) Modelling a friction damper: analysis of the experimental data and comparison with numerical results. ESDA, Turin
7. Firrone CM, Zucca S (2011) Modelling friction contacts in structural dynamics and its application to turbine bladed disks. In: Awrejcewicz J (ed) Numerical analysis—theory and application, pp 301–334. INTECH, Rijeka
8. Cattaneo C (1938) Sul contatto di due corpi elastici: distribuzione locale degli sforzi. Accademia dei Lincei 6:P I; 342–348, P II; 434–436, P III; 474–478
9. Mindlin RD, Deresiewicz H (1953) Elastic spheres in contact under varying oblique forces. J Appl Mech 20:327–344
10. Griffin JH (1980) Friction damping of resonant stresses in gas turbine engine airfoils. J Eng Power 102:329–333
11. Menq C, Chidamparam P, Griffin J (1991) Friction damping of two-dimensional motion and its application in vibration control. J Sound Vib 144:427–447
12. Hertz H (1881) Ueber die Berührung fester elastischer Körper. Journal für die reine und angewandte Math (Crelle) 92:156–171
13. Mindlin RD, Manson WP, Osmer JF, Deresiewicz H (1951) Effects of an oscillating tangential force on the contact surfaces of elastic spheres. In: Proceedings of the 1st national congress of applied mechanics, pp 227
14. Johnson KL (1955) Surface interaction between two elastically loaded bodies under tangential forces. Proc Roy Soc, Ser A 20:531–548
15. Goodman L, Brown C (1962) Energy dissipation in contact friction: constant normal and cyclic tangential loading. J Appl Mech 29:17–22
16. Menq C, Bielak J, Griffin J (1985) The influence of microslip on vibratory response: a new microslip model. J Sound Vib 107:279–293
17. Gola MM, Gastaldi C (2014) Understanding complexities in underplatform damper mechanics. In: Proceeding of ASME turbo expo
18. Harris T (1991) Rolling bearing analysis, 3rd edn. Wiley, New York
19. Brändlein J (1999) Ball and roller bearings : theory, design, and application. Wiley, New York
20. Lavella M, Botto D, Gola M (2013) Design of a high-precision, at-on-at fretting test apparatus with hight temperature capability. Wear, ed. Elsevier, New York